A Practical Metric for Cold Plate Thermal Performance in Two-Phase Direct-to-Chip Cooling

Qingyang Wang, Serdar Ozguc, Richard W. Bonner III
Accelsius
Austin, TX, USA
qwang@accelsius.com

Abstract

The increasing chip-level and rack-level power densities in data centers have necessitated liquid cooling solutions, in which pumped two-phase (2P) direct-to-chip (DTC) cooling shows promising performance and attracts great attention. The cold plate used in a 2P DTC system is a critical component dictating the cooling performance of the system. The thermal performance of a cold plate for single-phase DTC cooling is commonly characterized by the case-to-fluid thermal resistance with the inlet temperature as the characteristic fluid temperature. For 2P DTC, a case-to-fluid thermal resistance R_{cf} has been used to describe cold plate thermal performance with the characteristic fluid temperature taken as the saturation temperature, or the weighted average fluid temperature considering both subcooled sensible heat and latent heat. In this work, we developed thermohydraulic analysis and showed that R_{cf} can fail to represent 2P cold plate thermal performance and result in faulty conclusions in certain conditions, where a lower thermal resistance value could associate with higher case temperature, given server-level and rack-level conditions unchanged. We proposed a case-to-outlet thermal resistance R_{co}, which incorporates the temperature rise caused by the 2P pressure drop. R_{co} is more practically accessible and physically accurate, making it a good performance metric for 2P cold plates in 2P DTC systems for data centers.

Keywords

two-phase cooling, direct-to-chip, cold plate, thermal resistance, data center

Nomenclature

A_{chip}	area of the chip, [m^2]
Bo	boiling number
$c_{p,l}$	liquid specific heat capacity, [J/kg K]
d_h	hydraulic diameter, [m]
F_K	a constant in the Kandlikar correlation
f	friction factor
G	mass flux, [kg/m^2 s]
H_{ch}	channel height, [m]
h	heat transfer coefficient, [W/m^2 K]
h_{fg}	latent heat of vaporization, [J/kg]
k	thermal conductivity, [W/m K]
L	length, [m]
m	fin parameter, [m^{-1}]
$\dot{m}$	mass flow rate, [kg/s]
N_{ch}	number of channels
Nu	Nusselt number
P	pressure, [Pa]
Q	heat/power, [W]
q''_{fp}	footprint heat flux, [W/m^2]
q''_w	wall heat flux, [W/m^2]
R	thermal resistance, [K/W]
R_{cf}	case-to-fluid thermal resistance, [K/W]
R_{co}	case-to-outlet thermal resistance, [K/W]
Re	Reynolds number
T	temperature, [°C]
T_{case}	case temperature, [°C]
T_f	fluid average temperature, [°C]
t_{base}	base plate thickness, [m]
u	velocity, [m/s]
W_{ch}	channel width, [m]
W_{fin}	fin width, [m]
x	vapor quality

Greek symbols

ΔP	pressure drop, [Pa]
η	fin efficiency
μ	viscosity, [Pa·s]
ρ	density, [kg/m^3]

Subscripts

ac	acceleration component
ave	average between inlet and outlet
boil	boiling heat transfer process
CBD	convective boiling dominant
Cu	copper
ch	channel
fr	friction component
in	inlet of the cold plate
l	liquid phase
lat	latent heat part
le	liquid only
m	mean value for two-phase mixture
NBD	nucleate boiling dominant
nom	nominal
out	outlet of the cold plate
sat	saturation condition
sen	sensible heat part
tot	total heat
v	vapor phase

Acronyms

1P	single-phase
2P	two-phase
AI	artificial intelligence
CDU	coolant distribution unit
CP	cold plate
CPU	central processing unit
DTC	direct-to-chip

GPU	graphics processing unit
GWP	global warming potential
HTC	heat transfer coefficient
QD	quick-disconnect
TDP	thermal design power
TIM	thermal interface material

1. Introduction

The rapidly developing artificial intelligence (AI) technology has posed serious challenges to the thermal management of data centers, where traditional air convective cooling is no longer able to cope with the increasing thermal design power (TDP) from advanced processors and AI accelerators in densely populated server racks. Liquid cooling solutions are considered inevitable to keep up with the soaring cooling demand, among which two-phase (2P) direct-to-chip (DTC) cooling shows great promise. 2P DTC cooling offers high heat transfer potential using the latent heat of a dielectric refrigerant, requiring lower flow rate while ensuring no disastrous damage to IT equipment in case of leakage.

2P cooling has been extensively studied in the academic community. The forms of liquid-vapor phase change employed include pool boiling [1], flow boiling [2], thin film evaporation [3], spray cooling [4], and jet impingement [5]. Significant enhancements in heat transfer have been demonstrated using both water and dielectric fluids, with demonstrated heat flux dissipation approaching or exceeding 1 kW/cm^2 [6-8]. Due to its high performance, 2P heat transfer has been employed by thermal engineers for data centers. Compared with 2P immersion, 2P DTC allows retrofitting of existing data centers while still offering the high performance of 2P heat transfer.

A number of publications already exist for 2P DTC cooling for data centers. Heydari et al. [9] evaluated cold plates and cooling loops using experiments and models and provided suggestions on design considerations for 2P DTC cooling. Heydari et al. [10] analyzed the performance of different refrigerants for 2P DTC cooling and discussed the effects of different operating conditions. Wang et al. [11] established an experimental system for server-level 2P DTC characterization and demonstrated low thermal resistance up to a TDP of 1000 W using R1233zd(E). Ozguc et al. [12] modeled the rack-level flow distribution and demonstrated successful 2P flow control through the implementation of flow restrictors. Narayanan et al. [13] demonstrated high-performance cooling using 2P DTC with R1233zd(E) for a high-power GPU thermal test vehicle with a TDP of up to 2.2 kW. Wang et al. [14] conducted experiments at the cold plate-level and compared the performance of R1233zd(E) and R515B for 2P DTC cooling on different thermal test vehicles. Kulkarni et al. [15] and Wang et al. [16] introduced the concept of using a universal cold plate for both single-phase (1P) and 2P DTC cooling and demonstrated better thermal performance of 2P than 1P, suggesting that a faster and cheaper adoption of 2P DTC technology with existing 1P DTC infrastructure is possible.

For 1P DTC cooling, the case-to-fluid thermal resistance of a cold plate is widely used as the performance metric to evaluate cold plates, where the characteristic fluid temperature is taken as the cold plate inlet temperature. On the contrary, since 2P DTC for data center cooling is still in its infancy, there is no unanimously accepted performance metrics for 2P cold plates in data center thermal management. Many prior works used the saturation temperature to calculate the case-to-fluid thermal resistance [11, 13-16]. In this work, we provide analysis of some exemplary 2P cold plates, and show that the case-to-fluid thermal resistance defined using the saturation temperature (or the average temperature considering both 1P and 2P) could fail to represent 2P cold plate performance under certain conditions, with a lower resistance potentially leading to worse performance. We propose a case-to-outlet thermal resistance to serve as the performance metric for 2P cold plates, which incorporates the pressure drop of 2P flow in the cold plate. This metric correctly represents cold plate performance under given server-level and system-level conditions, and is easily accessible during cold plate testing. This allows data center engineers to quickly and accurately evaluate 2P cold plates during product development and product comparison, especially for people without a 2P thermal background, and helps to bridge the gap between 2P heat transfer research and data center cooling applications.

2. 2P DTC Fundamentals

Recently, Kulkarni et al. gave a comprehensive introduction and discussion of the 2P DTC cooling systems for data center thermal management [17]. The main components of a 2P coolant distribution unit (CDU) include the pump, the condenser, the reservoir, and the tubes, hoses, and fittings (including the quick-disconnect (QD) fittings) connecting all the components. Compared with a 1P DTC CDU, a refrigerant reservoir is added into a 2P DTC system to accommodate the volume expansion during heat load variations due to vastly different densities between liquid and vapor. The CDU can be in-rack or in-row, providing cooling for a single rack or for multiple racks, respectively. The CDU can also use liquid, air, or another circulated refrigerant as the coolant for the condenser. The different forms of 2P CDUs do not affect the analysis of this work, and an in-rack refrigerant to liquid CDU is employed in this work as an example.

The basic flow diagram of an in-rack 2P DTC system for data center cooling is shown in Figure 1. During operation, both vapor and liquid phases coexist in the reservoir and the refrigerant remains saturated. The liquid refrigerant is pumped from the saturated reservoir into the liquid manifold, distributed into the servers populated in the rack, and delivered to the cold plates attached to the high-power processors (CPUs/GPUs/AI accelerators). The refrigerant dissipates the heat and vaporizes, and exits the cold plates in the form of

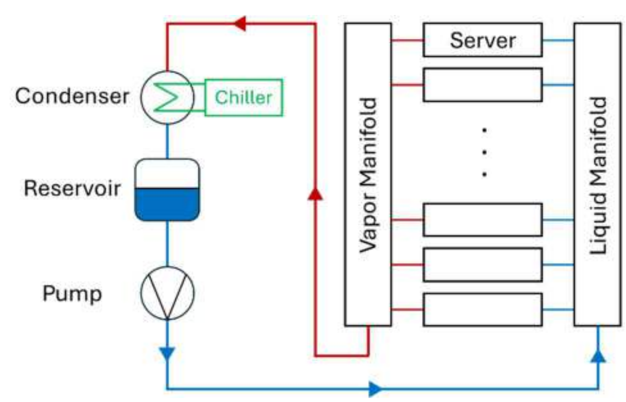

Figure 1. *Flow diagram of a 2P DTC system.*

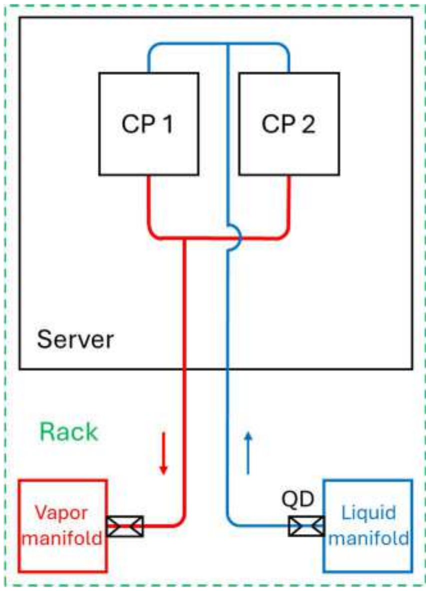

Figure 2. *Top view schematic of a two-processor server cooled in a 2P DTC system.*

liquid/vapor mixture. The saturated mixture enters the vapor manifold, and then gets condensed back into liquid and returns to the reservoir.

Figure 2 shows a top-view schematic of a server cooled in a 2P DTC system. For simplicity, the server is assumed to have two high-power processors. Within the server, the two cold plates (CPs) are hydraulically connected in parallel. The hoses delivering liquid into the server and taking saturated 2P mixture out of the server are interfaced with the liquid and vapor manifolds through QD couplings, which ensures spill-free and leak-free connection/disconnection of the flow paths without having to drain the refrigerant from any components.

3. Existing Performance Metric

Cold plates are one of the most important components dictating the thermal performance of a DTC system, either 1P or 2P. The thermal resistance of a cold plate is a representation of its cooling performance and is thus widely used as the performance metric for cold plates. The case-to-fluid thermal resistance is commonly used to describe cold plate performance, defined by the difference between the case temperature of the chip package and the characteristic fluid temperature divided by the dissipated total heat (the processor power). The case temperature can be taken as the maximum temperature across the case surface, the temperature at the center point of the case surface, or the average temperature across the case surface, depending on different applications and requirements.

The case-to-fluid thermal resistance, based on its definition, is a comprehensive lumped total resistance including contributions from thermal interface materials (TIMs) and base plate conduction. For 1P DTC systems, the characteristic fluid temperature is taken as the inlet coolant temperature T_{in}. However, in a 2P cold plate, liquid-vapor phase change process occurs under the constant saturation temperature T_{sat}. The inlet fluid is usually subcooled with $T_{in} < T_{sat}$. As 1P contribution in 2P cold plates is usually small, it is not thermally reasonable to use T_{in} in thermal resistance calculation for 2P.

The heat transfer in a 2P cold plate can be divided into two processes: 1) subcooled liquid absorbs heat as 1P liquid to raise its temperature from T_{in} to T_{sat}; 2) saturated liquid absorbs heat and transitions into vapor under T_{sat}. Consequently, the characteristic fluid temperature in the cold plate can be calculated as the energy-weighted average of these two processes:

$$T_f = \frac{Q_{sen}}{Q_{tot}} \frac{T_{in} + T_{sat}}{2} + \frac{Q_{lat}}{Q_{tot}} T_{sat} \tag{1}$$

where $Q_{tot} = Q_{sen} + Q_{lat}$. For a given refrigerant mass flow rate $\dot{m}$, the 1P sensible heat contribution Q_{sen} is

$$Q_{sen} = \dot{m} c_{p,l} (T_{sat} - T_{in}) \tag{2}$$

and the latent heat contribution Q_{lat} is

$$Q_{lat} = \dot{m} x_{out} h_{fg} \tag{3}$$

where x_{out} is the outlet vapor quality of the saturated mixture. A large vapor quality close to 1 ensures minimized pumping power, but could result in low thermal performance and potential dry-out. On the other hand, as 2P boiling usually has much higher heat transfer coefficient (HTC) than 1P convection, a small vapor quality indicates excessive flow rate and unwanted large 1P contribution. The designed vapor quality for a 2P cold plate is usually ~0.7 to avoid dry-out and flooding simultaneously.

With the characteristic fluid temperature T_f defined, the case-to-fluid thermal resistance for 2P cold plates is obtained as

$$R_{cf} = \frac{T_{case} - T_f}{Q_{tot}} \tag{4}$$

In the designed working conditions when 2P process dominates over 1P, T_f is very close to T_{sat} (usually within 1 °C), and given the much larger temperature difference between T_{case} and T_{sat} (>20 °C), it is convenient to use T_{sat} to replace T_f in Eq. (4) without introducing any significant error.

4. Model

4.1. Model formulation

Here we establish a model with classical correlations to analyze the performance of a set of microchannel-based 2P cold plates. To compare the thermal performance of different cold plates in a 2P DTC system, the chip-level, server-level, and rack-level conditions should all be maintained the same. The chip-level heating power and the form factor of the heating surface are fixed. The cold plates have the same mass flow rate. Given fixed CDU design, server plumbing, and operating conditions, the facility water temperature and flow rate determine the temperature/pressure of the saturated liquid in the reservoir as well as the pressure drop from the outlet of the cold plates to the reservoir. Consequently, the cold plate inlet temperature T_{in} (equal to the reservoir temperature) and outlet temperature/pressure for the saturated 2P mixture T_{out} and P_{out} are all fixed.

The 2P microchannel cold plates modeled here are used to cool a processor with a TDP of 2000 W. The processor has a form factor of 50×70 mm^2 and generates uniform heat flux on the case surface. The microchannel projected area matches the heated area, with the channel length L_{ch} matching the long edge of the chip surface. Figure 3 shows a drawing of the microchannel structures with the important geometrical

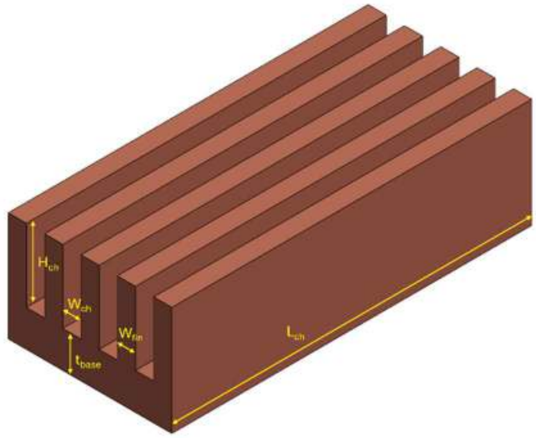

Figure 3. *Geometrical parameters of the microchannel cold plate in the model.*

parameters labeled. The channels are closed at the top and adjacent channels are sealed. The base plate thickness t_{base} is taken as 2.5 mm with a copper thermal conductivity of 390 W/mK, and the TIM thermal resistance R_{TIM} is taken as 10 mm^{2}K/W. The inlet fluid is subcooled at 35 °C, representing a simplified case when the facility cooling water outlet temperature is 35 °C and the CDU heat exchanger performs very efficiently. The outlet fluid is set as saturated 2P mixture at 45 °C, which is consistent with our rack-level experiments.

Refrigerant R1233zd(E) is employed as the working fluid. The thermophysical properties of the fluid are all evaluated at the outlet temperature of 45 °C and are assumed to be temperature independent. The mass flow rate of the cold plate is obtained by prescribing a nominal exit vapor quality x_{nom} of 0.7 for the given processor total power,

$$\dot{m} = \frac{Q_{tot}}{h_{fg} x_{nom}} \tag{5}$$

The nominal vapor quality ignores the 1P contribution. Given the channel geometrical parameters (Figure 3), the number of channels N_{ch} can be calculated based on the width of the processor. Uniform flow distribution is assumed such that the mass flow rate inside each channel is the same and can be calculated by $\dot{m}_{ch} = \dot{m}/N_{ch}$.

By assuming uniform heat flux on the processor surface, there are two segments along the flow length: a first 1P convection segment where subcooled liquid is heated to saturation pressure, and a second 2P flow boiling segment where saturated liquid vaporizes and the fluid exits the channels as a saturated liquid/vapor mixture. In the 2P segment, the flow is considered homogeneous and treated as 1P flow with 2P average properties. the 1P flow length L_{1P} is obtained as

$$L_{1P} = \frac{Q_{1P}}{Q_{tot}} L_{ch} \tag{6}$$

where Q_{1P} is the sensible heat,

$$Q_{1P} = \dot{m} c_{p,l} (T_{2P,in} - T_{in}) \tag{7}$$

$T_{2P,in}$ is the inlet temperature of the 2P segment, which is dependent on the pressure drop of the 2P segment. Consequently, an initial guess of $T_{2P,in} = T_{out}$ is taken to proceed the modeling with an iterated calculation until $T_{2P,in}$ is converged.

4.2. Channel pressure drop

The pressure drop along the channel is calculated by summing the 1P pressure drop and the 2P pressure drop. The 1P pressure drop is frictional, and given the small channel size, the flow is laminar, and the pressure drop can be calculated by the Darcy-Weisbach equation as

$$\Delta P_{1P} = \frac{L_{1P} f_{1P} \rho_l u_{1P}^2}{2 d_h} \tag{8}$$

where $u_{1P} = G_{ch}/\rho_l$ is the 1P flow velocity in the channel, $G_{ch} = \frac{\dot{m}_{ch}}{W_{ch} H_{ch}}$ is the channel mass flux. d_h is the channel hydraulic diameter, $f_{1P} = 64/Re_{1P}$ is the 1P laminar friction factor, $Re_{1P} = G_{ch} d_h/\mu_l$ is the 1P Reynolds number. It is noted that the constant value of 64 for fRe is valid for laminar flow in circular tubes, and value would be different for the rectangular channel shape here. Nonetheless, equations for circular tubes are implemented for simplicity, since 1P contribution is generally much smaller than 2P.

The 2P pressure drop in the channel includes friction and acceleration contributions. The friction pressure drop is obtained by

$$\Delta P_{2P,fr} = \frac{L_{2P} f_{2P} \rho_m u_{2P}^2}{2 d_h} \tag{9}$$

where $L_{2P} = L_{ch} - L_{1P}$ is the 2P flow length. For homogeneous 2P flow, the mixture density is calculated by

$$\rho_m = \left(\frac{x_{ave}}{\rho_v} + \frac{1 - x_{ave}}{\rho_l} \right)^{-1} \tag{10}$$

The average vapor quality in the 2P segment is $x_{ave} = x_{out}/2$, where the outlet vapor quality

$$x_{out} = \frac{Q_{2P}}{\dot{m} h_{fg}} = \frac{Q_{tot} - Q_{1P}}{\dot{m} h_{fg}} \tag{11}$$

The average 2P velocity is obtained by

$$u_{2P} = \frac{\dot{m}_{ch}}{\rho_m W_{ch} H_{ch}} \tag{12}$$

and the 2P friction factor f_{2P} is calculated depending on the flow type:

$$f_{2P} = \begin{cases} \dfrac{64}{Re_{2P}}, & \text{if } Re_{2P} \leq 2300 \\ (0.790 \ln Re_{2P} - 1.64)^{-2}, & \text{if } Re_{2P} > 2300 \end{cases} \tag{13}$$

where the average 2P Reynolds number is calculated by

$$Re_{2P} = \frac{G_{ch} d_h}{\mu_m} \tag{14}$$

in which the average mixture viscosity μ_m is obtained by

$$\mu_m = \left(\frac{x_{ave}}{\mu_v} + \frac{1 - x_{ave}}{\mu_l} \right)^{-1} \tag{15}$$

In most cases, $Re_{2P} < 2300$ and the flow is laminar due to the small channel size.

The 2P acceleration pressure drop in the channel can be calculated by

$$\Delta P_{2P,ac} = G_{ch}^2 \left(\frac{1}{\rho_{out}} - \frac{1}{\rho_l} \right) \tag{16}$$

where the outlet mixture density is calculated by

$$\rho_{out} = \left(\frac{x_{out}}{\rho_v} + \frac{1 - x_{out}}{\rho_l} \right)^{-1} \tag{17}$$

The outlet temperature is given, and the outlet fluid is saturated at T_{out} and P_{out}. Consequently, the inlet temperature of the 2P segment $T_{2P,in}$ can be obtained as the saturation temperature for the inlet pressure of the 2P segment $P_{2P,in}$, where

$$P_{2P,in} = P_{out} + \Delta P_{2P,fr} + \Delta P_{2P,ac} \tag{18}$$

and the obtained $T_{2P,in}$ is used to continue another iteration of calculation until convergence.

4.3. Channel heat transfer

Similar to pressure drop, the heat transfer characteristics in the channels are also based on the two-segment model. In the 1P segment, the convective HTC inside the channel is obtained by

$$h_{1P} = \frac{Nu_{1P} k_l}{d_h} \tag{19}$$

The 1P Nusselt number Nu_{1P} is taken as 4.36 for simplicity, which is the case for fully developed laminar flow inside a circular tube with constant wall heat flux.

In the 2P segment, the HTC can be estimated using the Kandlikar correlation [18]:

$$h_{2P} = \max(h_{NBD}, h_{CBD}) \tag{20}$$

where the nucleate boiling dominant and convective boiling dominant HTCs are calculated by

$$h_{NBD} = 0.6683 \left(\frac{\rho_l}{\rho_v}\right)^{0.1} x_{ave}^{0.16} (1 - x_{ave})^{0.64} h_{le} + 1058.0 Bo^{0.7} F_K (1 - x_{ave})^{0.8} h_{le} \tag{21}$$

$$h_{CBD} = 1.1360 \left(\frac{\rho_l}{\rho_v}\right)^{0.45} x_{ave}^{0.72} (1 - x_{ave})^{0.08} h_{le} + 667.2 Bo^{0.7} F_K (1 - x_{ave})^{0.8} h_{le} \tag{22}$$

Due to the laminar flow regime, the liquid only HTC h_{le} is equal to h_{1P}. The value of fluid-dependent parameter F_K is not available for R1233zd(E), and is taken as 1 in this work [19]. The boiling number Bo is defined by

$$Bo = \frac{q''_w}{G_{ch} h_{fg}} \tag{23}$$

Taking into consideration the fin efficiency, the wall heat flux q''_w is calculated as

$$q''_w = q''_{fp} \frac{W_{ch} + W_{fin}}{W_{ch} + 2\eta H_{ch}} \tag{24}$$

where the footprint heat flux is defined by

$$q''_{fp} = \frac{Q_{tot}}{A_{chip}} \tag{25}$$

with A_{chip} being the area of the processor (heated area). The fin efficiency is calculated by

$$\eta = \frac{\tanh(mH_{ch})}{mH_{ch}} \tag{26}$$

$$m = \sqrt{\frac{2h_{2P}}{k_{Cu} W_{fin}}} \tag{27}$$

where k_{Cu} is copper thermal conductivity (390 W/mK). The fin efficiency η is dependent on the 2P HTC, and an iteration is needed to converge the value.

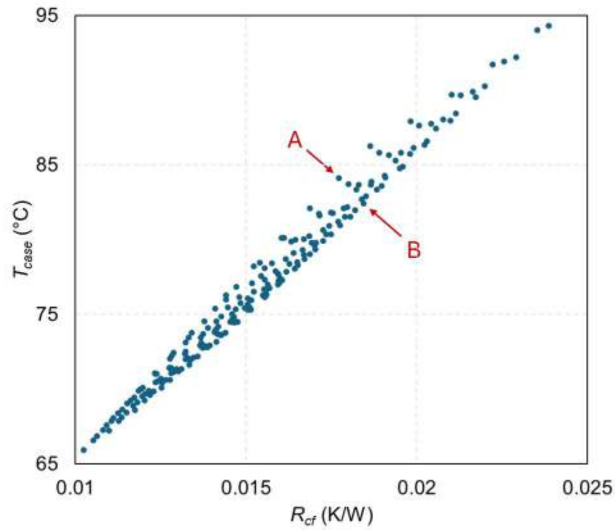

Figure 4. *Modeling results for different microchannel geometrical parameters.*

With the 1P and 2P HTCs obtained, the overall HTC along the channel wall is calculated as

$$h_{ch} = \left(\frac{Q_{1P}}{Q_{tot}} \frac{1}{h_{1P}} + \frac{Q_{2P}}{Q_{tot}} \frac{1}{h_{2P}}\right)^{-1} \tag{28}$$

The average case temperature is then obtained by

$$T_{case} = T_f + \frac{q''_w}{h_{ch}} + q''_{fp} \left(\frac{t_{base}}{k_{Cu}} + R_{TIM}\right) \tag{29}$$

where the characteristic fluid temperature T_f is given by

$$T_f = \frac{Q_{1P}}{Q_{tot}} \frac{T_{in} + T_{2P,in}}{2} + \frac{Q_{2P}}{Q_{tot}} \frac{T_{2P,in} + T_{out}}{2} \tag{30}$$

in which the T_{sat} in Eq. (1) is replaced by the average saturation temperature along the 2P segment.

5. Results and Discussion

Calculations are performed under different channel geometrical parameters. The fin width (0.15~0.25 mm), channel width (0.15~0.25 mm), and channel height (1~2 mm) are all swept for their respective ranges of values. Figure 4 shows the data points plotted as the case temperature against R_{cf}. In general, the case temperature increases with increasing R_{cf}, as expected. However, the trend is not monotonic, and for some cases, a lower R_{cf} would associate with a higher case temperature. For example, with $(W_{fin}, W_{ch}, H_{ch})$ = (0.23, 0.15, 1) mm for Point A in Figure 4, R_{cf} is 0.0177 K/W and T_{case} is 84.1 °C; whereas for the Point B, with geometries of (0.21, 0.25, 1.4) mm, R_{cf} is 0.0184 K/W and T_{case} is 82.4 °C. This indicates that R_{cf} could potentially give faulty conclusions when comparing two 2P cold plates under the exact same system-level conditions (with the same flow rate, the same subcooled inlet temperature, and the same outlet temperature). That is mainly because the fluid temperature T_f varies with different channel geometries, because the HTC and the pressure drop both increase with decreasing channel size. Consequently, in some cases, a smaller channel with a higher HTC could also have a higher saturation temperature in the

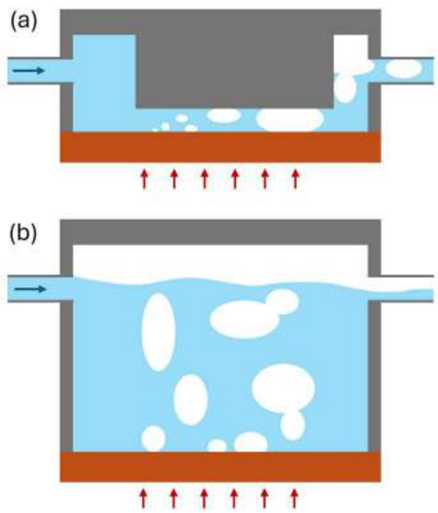

Figure 5. *(a) A microchannel flow boiling based cold plate with high pressure drop across the channels and the outlet manifold. (b) A pool boiling based cold plate with negligible internal pressure drop.*

channel given a constant outlet temperature, resulting in higher case temperature.

It is worth noting that the model is not aimed to be absolutely accurate to predict thermal performance of a cold plate. Instead, it is developed primarily to show that potential error exists in using R_{cf} to measure 2P cold plate performance. Therefore, the model is not numerically structured, simplified assumptions and correlations are used, and flow boiling instabilities are not considered. Moreover, the model neglects the pressure drop from outlet of the channels to the exit tube through an outlet plenum or manifold, which could be significant and result in more complexity in the pressure distribution. It is difficult to quantitatively model the pressure drop of the 2P flow with unknown flow pattern through a plenum/manifold with multi-dimensional shape. Nevertheless, it can be expected qualitatively that this pressure drop brings more possibility for R_{cf} defined by Eq. (4) to fail in describing thermal performance. For example, if two cold plates have the exact same boiling/convection HTC (and hence same R_{cf}), the one with higher outlet manifold pressure drop would have a higher characteristic fluid temperature in the channel, and consequently result in a higher processor case temperature. In an extreme case, as schematically shown in Figure 5, a microchannel based cold plate with very high pressure drops both along the channel and across the outlet (e.g., with a small neckdown to connect to a certain fitting) can have higher HTC and lower R_{cf} than a pool-boiling based cold plate with almost no pressure drop across itself, but can also have much higher fluid saturation temperature due to the pressure drop, and therefore potentially result in higher case temperature.

The modeling results above have shown that in a 2P system, the temperature distribution is not only dependent on temperature itself, but also on pressure. The case temperature is of most practical interest for thermal management purposes, and the outlet temperature is dictated by the server- and system-level operating conditions. Therefore, we propose a case-to-outlet thermal resistance R_{co}, defined by

$$R_{co} = \frac{T_{case} - T_{out}}{Q_{tot}} \tag{31}$$

Figure 6 shows the schematic drawing of the important temperature locations in a 2P cold plate, and the thermal resistance network. Similar to R_{cf}, R_{co} also includes contributions from TIM R_{TIM}, conduction across the base plate R_{cond}, and convective/boiling resistance within the cold plate R_{boil} (which may also include the subcooled 1P convection). Additionally, R_{co} also includes a thermal resistance R_{dp} resulted from fluid temperature reduction due to 2P pressure drop from the heat transfer surface to the outlet. Consequently, any rise of fluid characteristic temperature within the cold plate due to internal pressure drop of the 2P flow can be included within the R_{co} value. As discussed before, in a 2P DTC cooling system, T_{out} is determined by the system-level conditions, since it equals the reservoir fluid temperature plus the temperature drop both across the condenser and along the vapor return lines. Therefore, a higher R_{co} will always lead to a higher case temperature given fixed server- and rack-level conditions, making it a good performance indicator for 2P cold plates.

During the research and development phase of 2P cold plates, as well as evaluation and comparison of 2P cold plate products, experimental testing and performance characterization are conducted under conditions benefiting the implementation of R_{co}. For practical cold plate characterization, the local fluid temperature within the cold plate is usually not available, and imbedding additional temperature sensors inside the cold plate could be intrusive to affect the performance, or compromise the mechanical integrity under high internal pressure. Common tests are conducted with a temperature sensor placed outside of the cold plate, usually somewhere along the outlet tubing. Therefore, some prior characterizations [11, 13-16] of 2P cold plates reported case-to-fluid resistance R_{cf} while the reported values are in fact R_{co}. That means that the parameter R_{co} is not only accurate in capturing the true thermal performance considering the pressure drop contributions neglected before, but also practical in experimental testing and characterization of a cold plate by requiring no internal thermal sensor.

It is noted that the error caused by using R_{cf} most likely occurs when the system uses low-pressure refrigerants (such as

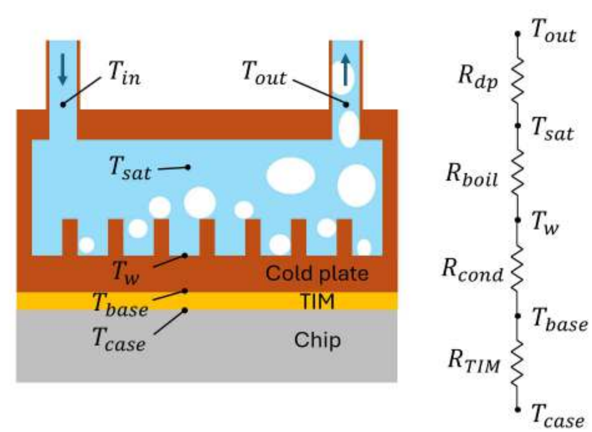

Figure 6. *Schematic drawing and thermal resistance network of a 2P DTC cold plate.*

R1233zd(E) used in this work) with high-power cooling, since the pressure drop is significant with small vapor density and large flow rate. When medium- to high-pressure refrigerants are used, the pressure drop inside cold plates can become minimal, so that $T_{out} \approx T_{sat}$ and R_{cf} value is approaching R_{co} (see Figure 6). Consequently, using R_{cf} might only result in negligible differences. For example, if we arbitrarily consider a 3 °C case temperature rise caused by R_{dp} to be a significant deterioration of performance, that translates to a 3 °C temperature drop from T_{sat} to T_{out}. Given a T_{out} of 45 °C, it corresponds to a ~3 psi pressure drop from the boiling site to the outlet for R1233zd(E), which is not impossible if the cold plate is not optimized (e.g. with long flow paths and narrow flow passages; complicated outlet manifold; neck-down at the outlet, etc.) and when high TDP requires large flow rate. However, for the same 3 °C temperature drop, the corresponding pressure drop for R515B (a medium-pressure refrigerant) becomes ~9 psi, which is highly unlikely for a reasonable cold plate design, especially since the larger vapor density of R515B already tends to produce smaller pressure drop given similar flow rate [14, 20]. Therefore, an estimation of the pressure drop within the cold plate based on refrigerant selection and working condition could be a quick and easy method to determine whether the proposed performance metric R_{co} is needed. When the pressure drop inside the cold plate can cause a rise of T_{case} larger than the threshold of tolerance, R_{co} will be needed to incorporate the pressure drop contribution and provide a fair evaluation of the performance. In other words, the necessity of using R_{co} is dependent on the refrigerant selection, designed flow rate, and the tolerance of temperature change due to cold plate pressure drop. Nonetheless, even when R_{co} does not result in material difference from R_{cf} and is not necessary, it is still easily accessible experimentally, since the outlet temperature is easier to obtain than the saturation temperature inside the cold plate.

It is also worth noting that the above discussion was based on a parallel configuration shown in Figure 2. When the cold plates are configured in series, the downstream cold plate receives a 2P mixture at its inlet, and the inlet manifold/plenum pressure drop could be significant, which increases the outlet temperature of the upstream cold plate given fixed rack-level conditions. In an exemplary case, if two downstream cold plates have different inlet 2P pressure drops, the same upstream cold plate will have different case temperatures. However, the situation described here does not contradict the analysis above. The pressure drop characteristics of the downstream cold plate should be viewed as a server-level feature when evaluating the upstream cold plate. Hence, the different case temperatures for the upstream cold plate should be attributed to the variation of server-level operating conditions instead of the cold plate itself.

6. Conclusions

With 2P cooling showing a promising future for data center thermal management, a performance metric for 2P cold plates is needed to compare cold plate performance and improve cold plate design [21]. In this work, we analyzed the thermal performance of microchannel 2P cold plates, and demonstrated that the case-to-fluid thermal resistance R_{cf} used in prior works based on saturation temperature can fail to represent the thermal performance of 2P cold plates. That is because the saturation temperature at which the fluid boils can be higher than the outlet fluid temperature determined by the system-level conditions, due to 2P pressure drop induced temperature reduction. Therefore, for 2P DTC cooling systems, we introduced a practical performance metric for 2P cold plates as the case-to-outlet thermal resistance R_{co}, which includes the thermal resistance related to internal pressure drop of the 2P flow. A higher R_{co} would always result in higher case temperature given fixed server- and system-level conditions, making it an accurate performance indicator for 2P cold plates, which is also easily accessible during cold plate testing. The R_{co} metric provides data center engineers with a quick method to evaluate cold plates in 2P DTC cooling, and reminds cold plate designers to take into consideration the pressure drop effect on thermal performance.

References

1. G. Liang, I. Mudawar. "Review of pool boiling enhancement by surface modification." International Journal of Heat and Mass Transfer 128 (2019): 892-933.
2. S. G. Kandlikar. "History, advances, and challenges in liquid flow and flow boiling heat transfer in microchannels: a critical review." Journal of Heat Transfer 134.3 (2012): 034001.
3. J. L. Plawsky, A. G. Fedorov, S. V. Garimella, H. B. Ma, S. C. Maroo, L. Chen, Y. Nam. "Nano-and microstructures for thin-film evaporation—A review." Nanoscale and microscale thermophysical engineering 18.3 (2014): 251-269.
4. J. Kim. "Spray cooling heat transfer: The state of the art." International Journal of Heat and Fluid Flow 28.4 (2007): 753-767.
5. L. Qiu, S. Dubey, F. H. Choo, F. Duan. "Recent developments of jet impingement nucleate boiling." International Journal of Heat and Mass Transfer 89 (2015): 42-58.
6. Q. Wang, and R. Chen. "Ultrahigh flux thin film boiling heat transfer through nanoporous membranes." Nano letters 18.5 (2018): 3096-3103.
7. K. P. Drummond, D. Back, M. D. Sinanis, D. B. Janes, D. Peroulis, J. A. Weibel, S. V. Garimella. "A hierarchical manifold microchannel heat sink array for high-heat-flux two-phase cooling of electronics." International Journal of Heat and Mass Transfer 117 (2018): 319-330.
8. C. Woodcock, C. Ng'oma, M. Sweet, Y. Wang, Y. Peles, J. Plawsky. "Ultra-high heat flux dissipation with Piranha Pin Fins." International Journal of Heat and Mass Transfer 128 (2019): 504-515.
9. A. Heydari, Y. Manaserh, A. Abubakar, C. Caceres, H. Miyamura, A. Ortega, J. Rodriguez. "Direct-to-Chip Two-Phase Cooling for High Heat Flux Processors." International Electronic Packaging Technical Conference and Exhibition. Vol. 86557. American Society of Mechanical Engineers, 2022.
10. A. Heydari, O. Al-Zu'bi, Y. Manaserh, M. Mehrabi, F. Hosseini, B. Sammakia. "System-Level Assessment of Green Refrigerant Replacements for Direct-to-Chip Two-Phase Cooling." 2024 23rd IEEE Intersociety Conference on Thermal and Thermomechanical Phenomena in Electronic Systems (ITherm). IEEE, 2024.

11. Q. Wang, S. Ozguc, A. Narayanan, R. W. Bonner. "A Server-Level Test System for Direct-To-Chip Two-Phase Cooling of Data Centers Using a Low Global Warming Potential Fluid", 2024 23rd IEEE Intersociety Conference on Thermal and Thermomechanical Phenomena in Electronic Systems (ITherm). IEEE, 2024.
12. S. Ozguc, Q. Wang, A. Narayanan, R. W. Bonner. "Investigation of Flow Restrictors for Rack Level Two-Phase Cooling Under Nonuniform Heating." 2024 40th Semiconductor Thermal Measurement, Modeling & Management Symposium (SEMI-THERM). IEEE, 2024.
13. A. Narayanan, Q. Wang, S. Ozguc, R. W. Bonner. "Investigation of Server Level Direct-to-Chip Two-Phase Cooling Solution for High Power GPUs", International Electronic Packaging Technical Conference and Exhibition. Vol. 88469. American Society of Mechanical Engineers, 2024.
14. Q. Wang, A. Narayanan, S. Ozguc, J. D. Moore, R. W. Bonner. "Performance Comparison of R1233zd(E) and R515B for Two-Phase Direct-to-Chip Cooling", 2025 24th IEEE Intersociety Conference on Thermal and Thermomechanical Phenomena in Electronic Systems (ITherm). IEEE, 2025.
15. D. Kulkarni, J. Gulick, J. King, B. Jarrett, P. George, Y. Feldman. "Thermal Performance of Common Cold Plate for Pumped Single- and Two-Phase Direct Liquid Cooling for Next Generation High Power Server Processors", International Electronic Packaging Technical Conference and Exhibition. Vol. 88469. American Society of Mechanical Engineers, 2024.
16. Q. Wang, D. P. Kulkarni, R. W. Bonner, J. C. Gulick. "Universal Direct-to-Chip Cold Plates for Single- and Two-Phase Cooling", OCP Global Summit 2024 Future Technologies Symposium.
17. D. Kulkarni, R. Tipton, E. Leka, J. Bankston, Q. Wang. "2P Refrigerant-Based Direct Liquid Cooling (DLC) Technology for Next Generation AI Clusters with High TDP Accelerators", OCP White Paper.
18. S. G. Kandlikar. "Heat transfer mechanisms during flow boiling in microchannels." Journal of Heat Transfer 126.1 (2004): 8-16.
19. V. P. Carey. *Liquid-vapor phase-change phenomena: an introduction to the thermophysics of vaporization and condensation processes in heat transfer equipment.* CRC Press; 2020 Feb 28.
20. R. Tipton, A. Wise, S. Mutabdzija, C. Shores, D. Kulkarni. "Maturation of Pumped Two-Phase Liquid Cooling to Commercial Scale-Up Deployment." International Electronic Packaging Technical Conference and Exhibition. Vol. 88469. American Society of Mechanical Engineers, 2024.
21. S. Ozguc, Q. Wang, A. Narayanan, J. D. Moore, R. W. Bonner. "Design Optimization of Manifold Integrated Skived Cold Plates for Two-Phase Flow-Boiling." 2025 41st Semiconductor Thermal Measurement, Modeling & Management Symposium (SEMI-THERM). IEEE, 2025.